Research

New Phytologist

The Fng3 ING protein regulates H3 acetylation and H4 deacetylation by interacting with two distinct histone-modifying complexes

Huaijian Xu[1]*, Meng Ye[1]*, Aliang Xia[1]*, Hang Jiang[2], Panpan Huang[1], Huiquan Liu[1], Rui Hou[3], Qinhu Wang[1], Dongao Li[1], Jin-Rong Xu[4] and Cong Jiang[1]

[1]State Key Laboratory of Crop Stress Biology for Arid Areas and NWAFU-Purdue Joint Research Center, College of Plant Protection, Northwest A&F University, Yangling, Shaanxi 712100, China; [2]Institution of Plant Protection, Shandong Academy of Agricultural Sciences, Jinan, Shandong 250100, China; [3]College of Forestry, Guizhou University, Guiyang 550025, China; [4]Department of Botany and Plant Pathology, Purdue University, West Lafayette, IN 47907, USA

Author for correspondence:
Cong Jiang
Email: cjiang@nwafu.edu.cn

Received: *10 February 2022*
Accepted: *30 May 2022*

New Phytologist (2022) **235:** 2350–2364
doi: 10.1111/nph.18294

Key words: *Fusarium graminearum*, histone acetylation, histone deacetylation, ING protein, pathogenesis, phytopathogenic fungus, wheat head blight.

Summary

- The steady-state level of histone acetylation is maintained by histone acetyltransferase (HAT) and histone deacetylase (HDAC) complexes. INhibitor of Growth (ING) proteins are key components of the HAT or HDAC complexes but their relationship with other components and roles in phytopathogenic fungi are not well-characterized.
- Here, the *FNG3* ING gene was functionally characterized in the wheat head blight fungus *Fusarium graminearum*. Deletion of *FNG3* results in defects in fungal development and pathogenesis. Unlike other ING proteins that are specifically associated with distinct complexes, Fng3 was associated with both NuA3 HAT and FgRpd3 HDAC complexes to regulate H3 acetylation and H4 deacetylation.
- Whereas FgNto1 mediates the FgSas3–Fng3 interaction in the NuA3 complex, Fng3 interacted with the C-terminal region of FgRpd3 that is present in Rpd3 orthologs from filamentous fungi but absent in yeast Rpd3. The intrinsically disordered regions in the C-terminal tail of FgRpd3 underwent phase separation, which was important for its interaction with Fng3. Furthermore, the ING domain of Fng3 is responsible for its specificities in protein–protein interactions and functions.
- Taken together, Fng3 is involved in the dynamic regulation of histone acetylation by interacting with two histone modification complexes, and is important for fungal development and pathogenicity.

Introduction

The INhibitor of Growth (ING) family members are evolutionarily conserved proteins with orthologs identified from yeast to human (He *et al.*, 2005). ING1 was originally isolated as a type II tumor suppressor, and decreased expression and mutations in ING1 have been detected in a variety of tumor cells (Gong *et al.*, 2005). Other ING proteins in mammals also play important roles in various cellular processes, including cell proliferation, apoptosis, hormone responses, DNA damage and chromatin remodeling (He *et al.*, 2005). In general, ING proteins are associated with the histone acetyltransferase (HAT) or deacetylase (HDAC) complexes to regulate various important biological processes in eukaryotic organisms. Although they are high similarity in sequences, ING proteins tend to interact with different histone-modifying complexes for chromatin and gene expression regulation.

Fungal ING genes are best studied in the budding yeast *Saccharomyces cevevisiae* (Loewith *et al.*, 2000). The three yeast ING proteins, Yng1, Yng2 and Pho23, are associated with the HAT or HDAC complexes, establishing a direct relationship between ING proteins and post-translational modifications of histones (Loewith *et al.*, 2000; Loewith *et al.*, 2001). Yng1, a stable component of the yeast NuA3 HAT complex, mediates the interaction of the NuA3 complex with nucleosomes for histone H3 acetylation (Howe *et al.*, 2002). Yng2, another yeast ING protein, interacts physically with the NuA4 subunit Epl1 to regulate NuA4 HAT activity and affect global H4 acetylation (Choy *et al.*, 2001). Expression of human ING1 in yeast suppresses the defects of the *yng2* mutant, suggesting a functional conservation between yeast and human ING proteins (Nourani *et al.*, 2003). Unlike Yng1 and Yng2, Pho23 is not associated with histone acetyltransferases but is a component of the Rpd3L HDAC complex (Loewith *et al.*, 2001). Pho23 and Rpd3 are functionally related in regulating the silencing of the rDNA and telomeric regions as well as mating-type loci (Loewith *et al.*, 2001). The

*These authors contributed equally to this work.

rpd3 and *pho23* deletion mutants are defective in *PHO5* expression and hypersensitive to cycloheximide and heat shock (Loewith *et al.*, 2001). The fission yeast has only two ING proteins, Png1 and Png2 (Chen *et al.*, 2010). Similar to Yng2, Png1 is associated with the NuA4 HAT complex and plays a critical role in cell growth and DNA damage response (Chen *et al.*, 2010; Greenstein *et al.*, 2020). By contrast, Png2, which is homologous to Pho23, functions as a component of the Rpd3 HDAC complex, but does not impact H4 acetylation (Nicolas *et al.*, 2007; Chen *et al.*, 2010).

In fungal pathogens, there are only limited studies on ING genes. In human pathogen *Candida albicans*, the *yng2* deletion mutant is significantly reduced in H4 acetylation and exhibits growth and cell cycle defects (Lu *et al.*, 2008). In the filamentous ascomycete *Fusarium graminearum*, Fng1, an ortholog of yeast Yng2, specifically interacts with the FgEsa1 HAT of the NuA4 complex and deletion of *FNG1* results in a significant reduction in H4 but not H3 acetylation (H. Jiang *et al.*, 2020). The *fng1* mutant is defective in vegetative growth, conidiation, sexual reproduction, deoxynivalenol (DON) production and plant infection. Spontaneous suppressors with mutations in the key components of the Rpd3 complex, including orthologs of yeast Rpd3, Sin3 and Sds3, recovers the growth defect of the *fng1* mutant but not its defects in plant infection or sexual reproduction (H. Jiang *et al.*, 2020). Non-sense and frameshift mutations in *FgRPD3* reduce HDAC activities, which partially alleviates the defect of the *fng1* mutant in H4 acetylation. The FgRpd3 HDAC appears to have an antagonistic relationship with Fng1 and FgEsa1 HAT on regulating H4 acetylation in vegetative hyphae (H. Jiang *et al.*, 2020).

Fusarium graminearum, a homothallic (self-fertile) ascomycete, is a major causal agent of Fusarium head blight (FHB) in wheat and barley worldwide (Goswami & Kistler, 2004). In addition to severe yield losses, it is a producer of trichothecene mycotoxin DON that is a potent inhibitor of protein synthesis (Audenaert *et al.*, 2013; Chen *et al.*, 2019). Deoxynivalenol is not only harmful to human and animal health, but also plays a critical role in plant infection (Cuzick *et al.*, 2008). *Fusarium graminearum* overwinters and forms perithecia (sexual fruiting bodies) on plant debris (Ren *et al.*, 2022). In the spring, ascospores are forcibly discharged from the perithecia as the primary inoculum for airborne dispersal which infects wheat and barley florets during flowering (Trail, 2009; Imboden *et al.*, 2018). Plant infection is initiated with the differentiation of penetration structures known as compound appressoria and infection cushions by *F. graminearum* (Boenisch & Schafer, 2011). After penetration, morphologically irregular invasive hyphae grow intra- and intercellularly in infected plant tissues and spread from infested spikelets to neighboring ones via the rachis of the wheat head (Jansen *et al.*, 2005). As in other eukaryotic organisms, the acetylation of H3 and H4 plays critical roles in regulating stage-specific gene expression in this important plant pathogen (Connolly *et al.*, 2013; Wang *et al.*, 2021). Suppressor mutations in *FgRPD3* partially rescue the defects of the *fng1* mutant in growth and H4 acetylation during vegetative growth but have no effects on its defects in plant infection and sexual reproduction, suggesting that stage-specific regulation of H4 acetylation and gene expression in *F. graminearum* (H. Jiang *et al.*, 2020). Furthermore, because Fng1 is specific for the NuA4 complex and H4 acetylation and the *fng1* deletion mutant is normal in H3 acetylation, other ING proteins must be involved in the NuA3 complex and H3 acetylation. Like other ascomycetes, *F. graminearum* has orthologs of the key components of the NuA3 complex, including orthologs of yeast Sas3, Nto1 and Taf14. Deletion of the *FgSAS3* HAT gene results in defects in DON production and plant infection (Kong *et al.*, 2018).

In this study, we functionally characterized an ING gene named *FNG3* (FGRAMPH1_01T23021) in *F. graminearum*. Fng3 not only interacted with the catalytic subunit of NuA3 complex for the regulation of H3 acetylation, but also associated with FgRpd3 to regulate histone deacetylation. The interaction between Fng3 and FgRpd3 was mediated by the C-terminal tail of FgRpd3 that is present in its orthologs from various filamentous fungi but not in yeast Rpd3. Taken together, Fng3 plays a critical role in the regulation of fungal development and pathogenicity by interacting with two different histone modification complexes. It provides a novel model of interaction between ING proteins and histone-modifying complexes in *F. graminearum*.

Materials and Methods

Strains and culture conditions

The wild-type (WT) *Fusarium graminearum* strain PH-1 (Cuomo *et al.*, 2007) and mutants generated in this study (Supporting Information Table S1) were routinely cultured on potato dextrose agar (PDA) plates at 25°C. Growth rate and conidiation was assayed with 3-d-old PDA cultures and 5-d-old carboxymethyl cellulose (CMC) cultures as described (Hou *et al.*, 2002). Sexual reproduction was assayed on carrot agar cultures as described (Wang *et al.*, 2011). For selection of transformants, hygromycin B, geneticin and zeocin (Calbiochem, Germany) were added to the final concentration of 300, 200 and 400 μg ml^{-1}.

Generation of targeted gene deletion mutants

The *FNG3* gene replacement construct was generated with the split marker approach with primers listed in Table S2 (Zhou *et al.*, 2011). The resulting PCR products were transformed into protoplasts of PH-1 with the polyethylene glycol (PEG)-mediated transformation as described (Hou *et al.*, 2002). Transformants resistant to hygromycin B were screened by PCR for the deletion of *FNG3* and confirmed by PCR with both upstream and downstream anchor primers. Similar approaches were used to generate the *fng2* and *Fgnto1* deletion mutants.

Generation of green fluorescent protein or mCherry fusion constructs and transformants

In order to generate the *FNG3*- Generation of green fluorescent protein (GFP) fusion construct by the yeast gap repair approach

(Bruno *et al.*, 2004), the full-length *FNG3* gene with its promotor was amplified with primers listed in Table S2 and co-transformed with *Xho*I-digested pFL2 into yeast strain XK1-25 as described (Zhou *et al.*, 2011). The same approach was used to generate the *FgRPD3*-mCherry construct with primers listed in Table S2. Fungal transformants were verified by PCR for the transforming fusion constructs and examined for GFP or mCherry signals by epifluorescence microscopy (Jiang *et al.*, 2016).

Plant infection

Flowering wheat heads of wheat cultivar XiaoYan 22 plants were inoculated with 10 µl of conidium suspensions (10^5 spores ml^{-1}) and examined for disease symptoms as described (Gale *et al.*, 2007). The diseased wheat kernels were collected from the inoculation sites and assays for deoxynivalenol (DON) production using a GCMS-QP2010 system with the AOC-20i autoinjector (Jiang *et al.*, 2019). Infection cushion formation was examined with a JEOL 6360 scanning electron microscope (SEM) as described (Boenisch & Schafer, 2011). For infection assays wheat coleoptile assays (Zhang *et al.*, 2012), the top portion of wheat coleoptiles was excised and inoculated with 2 µl conidium suspensions (10^5 spores ml^{-1}) over the wound sites (Zhang *et al.*, 2012). Invasive hyphae grown inside plant tissues sampled at 2 d post-inoculation (dpi) were examined with epifluorescence microscopy after staining with Alexa Fluor 488 (Jiang *et al.*, 2019).

Assays for histone acetylation

Total proteins were isolated from vegetative hyphae harvested from 24 h YEPD cultures as described previously (Jiang *et al.*, 2016). For Western blot analyses, total proteins were separated on 12.5% SDS-PAGE gels and transferred to nitrocellulose membranes (Zhou *et al.*, 2012). H3 and H4 acetylation was detected with Abcam antibodies specific for H3K4ac (ab176799), H3K9ac (ab10812), H3K14ac (ab52946), H3K18ac (ab1191), H3K27ac (ab45173), H3K36ac (ab177179), H4K5ac (ab51997, H4K8ac (ab15823), H4K12ac (ab46983) and H4K16ac (ab194352). Detection with the anti-Histone H3 (ab209023) and anti-Histone H4 (ab10158; Abcam, Cambridge, UK) antibodies were used as the loading controls (H. Jiang *et al.*, 2020).

Yeast-two-hybrid and bimolecular fluorescence complementation assays

In order to detect protein–protein interactions based on yeast-two-hybrid (Y2H) assays, full-length cDNAs or fragments of genes were amplified and cloned into the pGADT7 prey or pGBKT7 bait vector (TaKaRa Bio, Tokyo, Japan) (Liu *et al.*, 2015). The resulting bait and prey constructs were transformed in pairs into yeast strain AH109 and assayed for growth on SD-Trp-Leu-His plates as described previously (Liu *et al.*, 2015). For bimolecular fluorescence complementation (BiFC) assays, genes were amplified and cloned into the pHZ65 vector and pHZ68 vector, respectively (Zhao & Xu, 2007). Transformants resistant to hygromycin and zeocin were verified by PCR and examined for yellow fluorescent protein (YFP) signals by epifluorescence microscopy after staining with 4,6-diamidino-2-phenylindole (DAPI) as described (Liu *et al.*, 2015).

RNA-seq, chromatin immunoprecipitation-seq and quantitative reverse transcription-PCR assays

Total RNAs isolated from hyphae harvested from 24 h YEPD cultures of the WT and *fng3* deletion mutant were sequenced with Illumina HiSeq 2500 at Novogene Bioinformatics Technology (China). Differential expression analysis of genes was performed using the EDGERUN package (Dimont *et al.*, 2015) with the exactTest function. RNA-seq data generated in this study were deposited in the NCBI SRA database under accession numbers SRR17659995-SRR17660003 and SRR19214415-SRR19214418. Chromatin immunoprecipitation (ChIP) assays were performed by Wuhan Igenebook Biotechnology with hyphae harvested from 24 h YEPD cultures of the WT PH-1 stain as described (H. Jiang *et al.*, 2020). The ChIP-seq data generated in this study were deposited in the NCBI SRA database under accession number SRR19414282-SRR19414283. RNA samples of the WT and *fng3* mutant were isolated from hyphae harvested from 24 h YEPD cultures and assayed for transcription levels with the CFX96 Real-Time System (Bio-Rad) as described previously (H. Jiang *et al.*, 2020). *Fusarium graminearum* actin gene FGRAMPH1_01G24551 was used as the internal control (H. Jiang *et al.*, 2020).

Phase separation assays

For *in vivo* phase separation assays, hyphae of *FgRPD3*^{CT}-GFP transformants were cultured in YEPD for 12 h and examined by fluorescent microscopy with a FV3000 microscope (Olympus, Tokyo, Japan). For *in vitro* phase separation assays, FgRpd3^{CT}-GFP-HIS fusion proteins were expressed in *E. coli* strain BL21 and purified with Ni NTA agarose beads (Smart-Lifesciences Biotechnology, Changzhou, China) as described previously (C. Jiang *et al.*, 2020). After dialysis in the elution buffer (50 mM NaH_2PO_4, 300 mM NaCl, 250 mM imidazole, pH 8.0) (Chen *et al.*, 2020), purified recombinant proteins were diluted to the desired concentrations in the droplet formation buffer with or without 10% PEG8000 as described previously (Chen *et al.*, 2020). Droplet formation then was examined with an Olympus FV3000 microscope.

Fluorescence recovery after photobleaching analysis

In order to capture the dynamics of FgRpd3^{CT}-GFP proteins in solution, fluorescence recovery after photobleaching (FRAP) was carried out with an Olympus FV3000 laser scanning confocal microscope. Two scan images were captured before bleaching and a single body was bleached using 3% power with 488-nm and laser lines for 1 s. Time-lapse images were collected at 1-s intervals. The raw data were processed and analyzed with

EasyFRAP-web and GraphPad Prism (Koulouras *et al.*, 2018; Chen *et al.*, 2020). For each sample, the pre-bleaching fluorescence intensity was arbitrarily set to 1.

Results

Fng3, but not Fng2, is part of the NuA3 HAT complex

Besides Fng1, that is associated with the NuA4 complex, two other predicted genes in the *F. graminearum* genome, FGRAMPH1_01T00795 and FGRAMPH1_01T23021 (named *FNG2* and *FNG3*, respectively), also encode ING proteins with an N-terminal ING domain and a C-terminal PHD finger domain. Comparative analysis with 31 representative species of Ascomycota, Basidiomycota, Mucoromycota and Chytridiomycota (Table S3) showed that orthologs of *FNG1* (including *S. cerevisiae* Yng2 and *S. pombe* Png1) and *FNG2* (including *S. cerevisiae* Pho23 and *S. pombe* Png2) are present in 29 of them and can be clustered into two distinct clades although their copy numbers vary among different fungi. Whereas all selected 16 Ascomycetes species have only one *FNG1* and one *FNG2* ortholog, six of 11 Basidiomycetes species have two *FNG2* orthologs although they also contain one *FNG1* ortholog (Fig. S1). Many Mucoromycetes and Chytridiomycetes species have more than two *FNG1* or *FNG2* orthologs, that may have originated from gene duplication events (Fig. S1). By contrast, orthologs of *FNG3* and *S. cerevisiae* Yng1 are only present in Ascomycetes species, and they belong to a separate clade from *FNG1* and *FNG2* orthologs (Fig. S1). None of the Basidiomycetes, Mucoromycetes and Chytridiomycetes species that we examined have *FNG3* orthologs, confirming the restrictive distribution of *FNG3* orthologs to Ascomycetes (Table S3; Fig. S1).

In order to determine their functional relationship with the NuA3 or NuA4 complex, we generated the *FNG2*-nYFP and *FNG3*-nYFP fusion constructs and transformed them in pairs with the *FgSAS3*-cYFP or *FgESA1*-cYFP fusion constructs into the WT strain PH-1 for BiFC assays. *FgSAS3* and *FgESA1* are orthologs of yeast *SAS3* and *ESA1* that encode the HAT of the NuA3 and NuA4 complexes, respectively. In transformants expressing both *FNG3*-nYFP and *FgSAS3*-cYFP fusion constructs, YFP signals were observed in the nucleus (Fig. 1a). However, YFP signals were not observed in the *FNG2*-nYFP *FgSAS3*-cYFP transformants. We also failed to observed YFP signals in transformants expressing *FgESA1*-cYFP together with *FNG2*-nYFP or *FNG3*-nYFP fusion constructs (Fig. 1b). These results indicated that only Fng3 interacts with FgSas3, the HAT of the NuA3 complex and neither Fng2 nor Fng3 interacts with FgEsa1, the HAT of the NuA4 complex. Therefore, Fng3 may function as the ING protein in the NuA3 complex in *F. graminearum*.

FgNto1 interacts with both FgSas3 and Fng3 in the NuA3 HAT complex

We then generated the full-length Fng3 bait construct and assayed its interaction with FgSas3 in Y2H assays. The direct interaction between Fng3 and FgSas3 was not detected (Fig. 1c), indicating that the interaction between Fng3 and FgSas3 may require other components of the NuA3 complex.

Besides FgSas3, there are two other conserved subunits of the NuA3 complex, FgTaf14 and FgNto1, in *F. graminearum*. In Y2H assays, Fng3 interacted with FgNto1 but not with FgTaf14 (Fig. 1c). The direct interaction also was observed between FgNto1 and FgSas3 (Fig. 1c). Therefore, FgNto1 interacts with both FgSas3 and Fng3, which may mediate the FgSas3–Fng3 interaction in the NuA3 HAT complex. To test this hypothesis, we deleted the *FgNTO1* gene (FGRAMPH1_01T24301) in the *FNG3*-nYFP *FgSAS3*-cYFP transformant. In the resulting *Fgnto1* mutant, growth rate was only slightly reduced (Fig. 1d) but YFP signals were no longer observed in the nucleus (Fig. 1e), indicating that deletion of *FgNTO1* disrupts the interaction between FgSas3 and Fng3 in *F. graminearum* (Fig. 1f).

The *fng3* deletion mutant is defective in H3 acetylation

In order to further characterize its role in the NuA3 HAT complex, we generated the *fng3* deletion mutant with the split marker approach (Zhou *et al.*, 2011). The *fng3* deletion mutant was normal in conidium morphology although it was slightly reduced in growth rate and conidiation (Fig. 2a,b). On mating plates, it still produced melanized perithecia but failed to form mature asci and ascospores (Fig. 2c). When assayed for the acetylation of histone H3 with the antibodies specific for H3K4ac, H3K9ac, H3K14ac, H3K18ac, H3K27ac and H3K36ac, the *fng3* mutant was significantly reduced in the acetylation level of H3K4ac, H3K14ac and H3K36ac in comparison with the WT (Fig. 2d), confirming the role of Fng3 in H3 acetylation. For comparison, we used the same gene replacement approach to generate the *fng2* deletion mutant. However, deletion of *FNG2*, an ortholog of yeast *PHO23*, had no significant effect on H3 acetylation (Fig. 2d), further confirming that Fng3, not Fng2, is the ING protein of the NuA3 complex in *F. graminearum*.

FNG3 is important for penetration and spreading of infectious growth

In infection assays with wheat heads, the *fng3* mutant was significantly reduced in virulence (Fig. 2e). It usually only caused FHB symptoms on the inoculated kernels, indicating that it was defective in spreading from the inoculation site to neighboring spikelets (Fig. 2e). Deoxynivalenol is phytotoxic and an important virulence factor in *F. graminearum* for spreading infectious growth through the rachis (Cuzick *et al.*, 2008). In infested wheat kernels, DON production was decreased > 5-fold in the *fng3* mutants in comparison with the WT (Fig. 2f). When examined by SEM, the *fng3* mutant had no obvious defects in infection cushion formation (Fig. 2g). However, in infection assays with wheat seedlings, the *fng3* mutant rarely successfully penetrated through wounding sites and had only limited infectious growth inside coleoptile cells adjacent to the wound sites (Fig. 2h). Transverse growth of invasive hyphae across neighboring cells was rarely observed although limited longitudinal growth was observed at some wounding inoculation sites (Fig. 2h). These

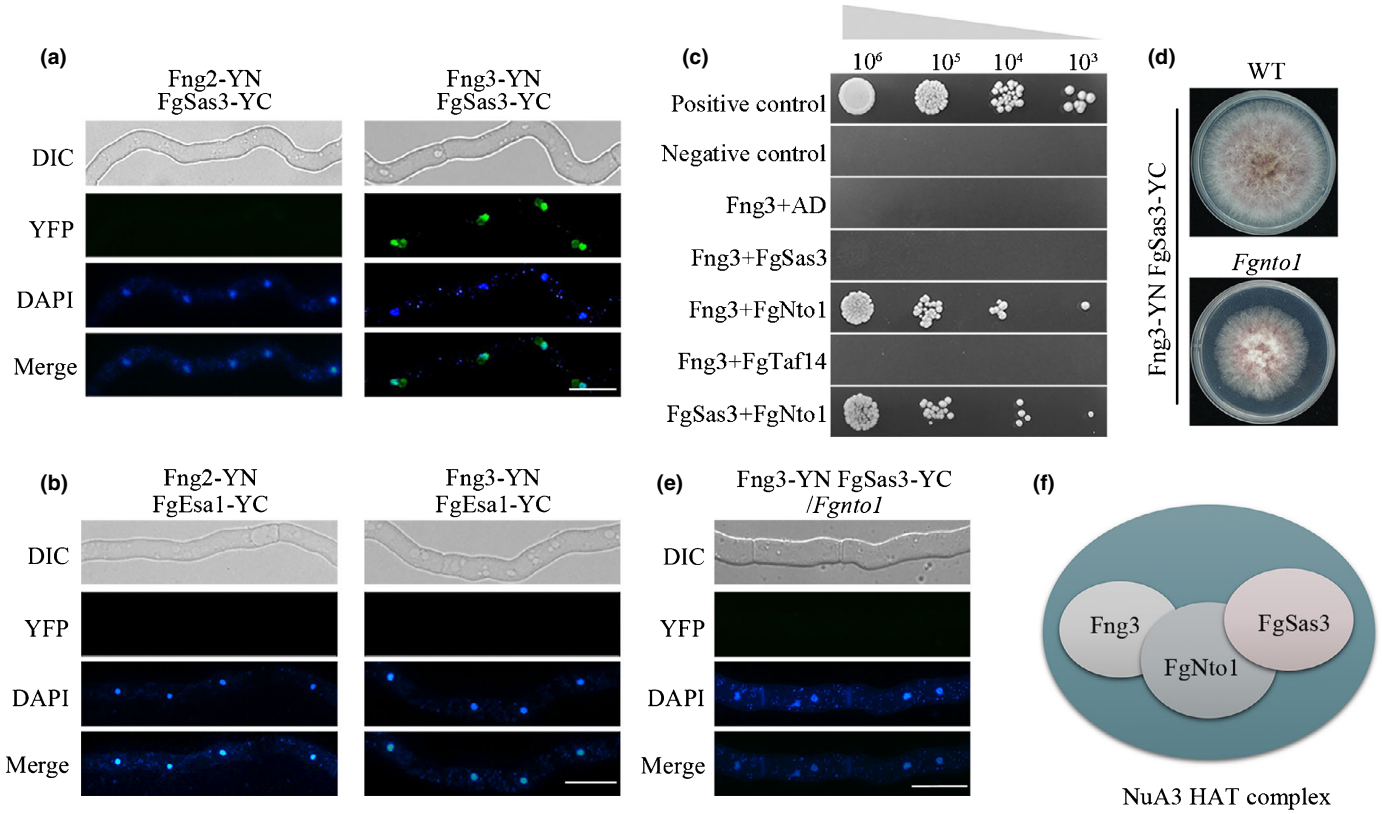

Fig. 1 Assays for the association of Fng3 with the NuA3 histone acetyltransferase (HAT) complex. (a) Bimolecular fluorescence complementation (BiFC) assays for the interaction of FgSas3 with Fng2 and Fng3. Germlings of the transformants expressing the *FgSAS3*-cYFP and *FNG2*-nYFP or *FNG3*-nYFP fusion constructs were stained with 4,6-diamidino-2-phenylindole (DAPI) and examined by epifluorescence microscopy (YFP, yellow fluorescent protein). Bar, 10 μm. (b) BiFC assays for the interaction of FgEsa1 with Fng2 and Fng3 in transformants expressing *FgESA1*-cYFP and *FNG2*-nYFP or *FNG3*-nYFP. Bar, 10 μm. (c) Different concentrations (cells ml^{-1}) of yeast transformants expressing the indicated bait and prey constructs were assayed for growth on SD-Trp-Leu-His plates. (d) Three-day-old PDA cultures of the wild-type (WT) and the *FgSAS3*-cYFP *FNG3*-nYFP and *Fgnto1 FgSAS3*-cYFP *FNG3*-nYFP transformants. (e) BiFC assays for the effect of *FgNTO1* deletion on the interaction of Fng3 with FgSas3. YFP signals were not observed in the *Fgnto1 FgSAS3*-cYFP *FNG3*-nYFP transformants. Bar, 10 μm. (f) Schematic drawing of interactions among Fng3, FgNto1 and FgSas3 in the NuA3 HAT complex.

results indicated that *FNG3* plays a crucial role in the penetration and spreading of infectious growth inside plant tissues.

For complementation assays, we generated the *FNG3*-GFP construct and transformed it into the *fng3* mutant. The resulting *fng3*/*FNG3*-GFP transformants were normal in vegetative growth, sexual reproduction and virulence (Fig. 2a–c,e,f). These results indicate that the expression of *FNG3*-GFP fully complemented the *fng3* mutant.

Fng3 co-regulates subsets of genes with Fng1 in vegetative hyphae

Histone acetylation is associated with gene expression. To determine the role of Fng3 in gene expression, we generated RNA-seq data with the *fng3* mutant. In comparison with the WT, a total of 2242 differentially expressed genes (DEGs) had >2-fold changes in their expression levels (Table S4). To verify RNA-seq data, we selected three DEGs upregulated and three DEGs downregulated in the *fng3* mutant for quantitative reverse transcription (qRT)-PCR assays. All of them had similar changes in their expression levels in the RNA-seq data and qRT-PCR results (Fig. S2). Among the 2242 DEGs, 1263 were downregulated in the *fng3* mutant. GO enrichment analysis showed that these downregulated DEGs were enriched for genes involved in nucleobase-containing compound biosynthetic process, regulation of gene expression and microtubule associated complex (Fig. S3). For the 979 DEGs upregulated in the *fng3* mutant, they were enriched for genes involved in oxidation–reduction process and transmembrane transport (Fig. S4).

We then compared the RNA-seq data of the *Fgsas3* and *fng3* mutants. Among the 1188 DEGs downregulated in the *Fgsas3* mutant, 365 also had decreased expression in the *fng3* mutant (Fig. 3a). Among the 1155 DEGs upregulated in the *Fgsas3* mutant, 330 of them also had increased expression levels in the *fng3* mutant (Fig. 3a), indicating that these genes are negatively regulated by both *FgSAS3* and *FNG3*.

The 365 DEGs downregulated in both *fng3* and *Fgsas3* mutants may be enriched for the direct or indirect targets of NuA3 HAT complex. In comparison with the random-selected genes, the 365 DEGs downregulated in both *fng3* and *Fgsas3* mutants were highly enriched in H3K14ac (acetylated by FgSas3) based on ChIP-seq data generated with the anti-H3K14ac antibody (Fig. S5a). The high level of H3K14ac enrichment in those genes probably is modulated by Fng3 and its related NuA3 HAT

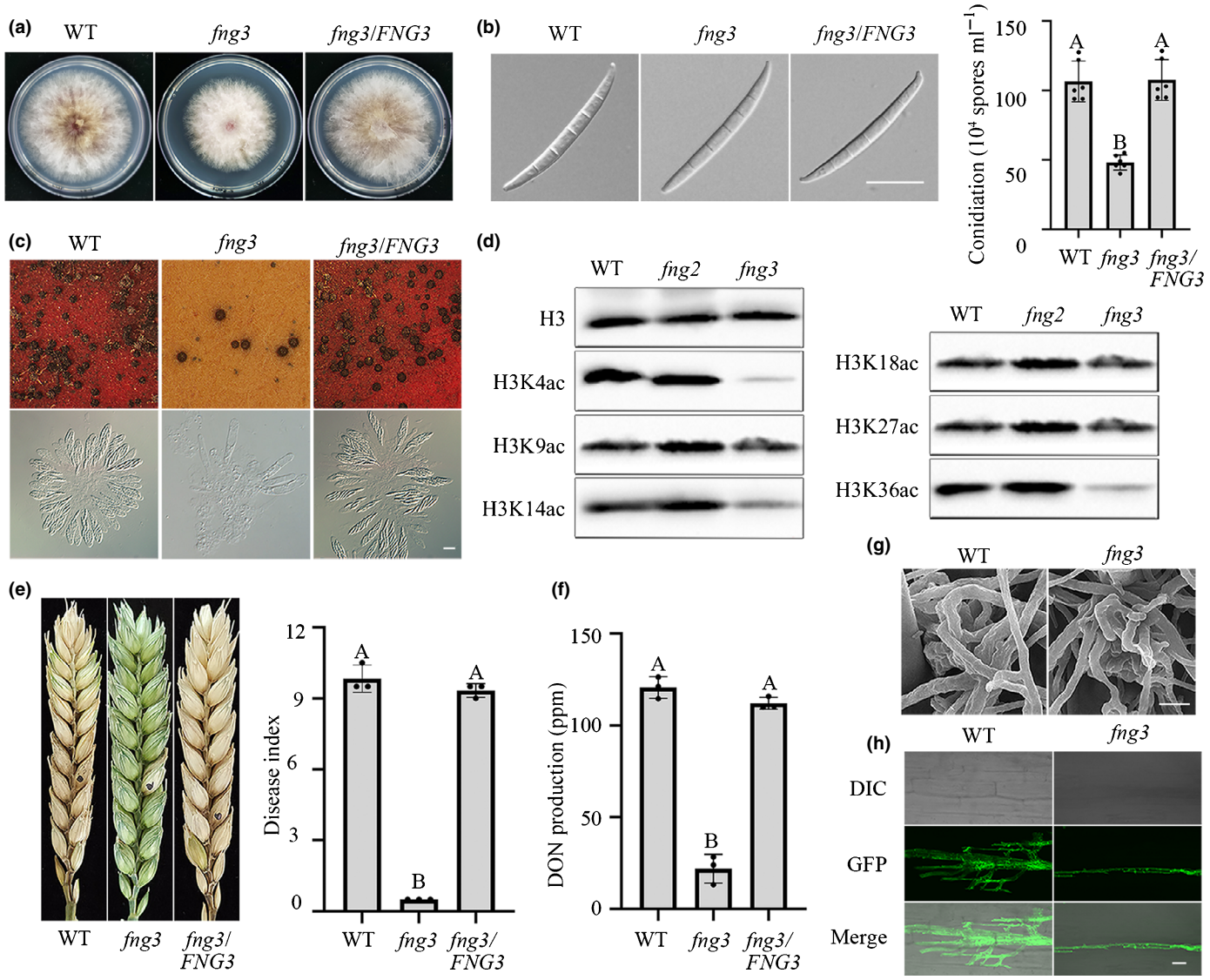

Fig. 2 Assays for the functions of *FNG3* in *Fusarium graminearum*. (a) Three-day-old potato dextrose agar (PDA) cultures of the wild-type (WT), fng3 mutant and fng3/FNG3 transformant. (b) Conidial morphology of the indicated strains (left panels). Bar, 20 μm. Conidiation of the indicated strains (right panels). Error bar represents SD from mean (marked with black dots on the bars) of six independent experiments. (c) Two-week-old mating cultures of the indicated strains were examined for perithecia (upper panels) and ascus development (lower panels). Bar, 20 μm. (d) Western blots of total proteins isolated from the WT and the fng2 and fng3 mutants were detected with the antibodies specific for H3K4ac, H3K9ac, H3K14ac, H3K18ac, H3K27ac and H3K36ac. (e) Wheat heads inoculated with the indicated strains (left panels) were examined for head blight symptoms at 14 d post-inoculation (dpi). Black dots mark the inoculated spikelets (left panels). The disease index of the indicated strains (right panels). Error bar represents SD from mean (marked with black dots on the bars) of three independent experiments with ≥ 10 wheat heads examined in each experiment. (f) Mean and SDs of deoxynivalenol (DON) levels in diseased wheat spikelets inoculated with the indicated strains based on data from three biological replicates. (g) Infection cushions formed on wheat lemma were examined by SEM under ×2000 amplification at 2 dpi. Bar, 10 μm. (h) Wheat coleoptiles infected with the indicated strains were examined for invasive hyphae at 2 dpi after staining with Alexa Fluor 488. Bar, 20 μm. For (b, e and f), different letters indicate significant differences based on ANOVA analysis followed by Duncan's multiple range test ($P = 0.05$).

complex. Gene ontology (GO) analysis revealed that they were enriched for genes involved in nucleic acid binding and transcriptional regulation (Fig. S5b).

Deletion of *FNG1* also affects the expression of 3546 genes in *F. graminearum* (H. Jiang *et al.*, 2020). We then compared the RNA-seq data of the *fng1* and *fng3* mutants. Among the 1263 DEGs downregulated in the *fng3* mutant, 502 of them also had decreased expression levels in the *fng1* mutant (Fig. 3b). In addition, 243 of the 979 DEGs upregulated in the *fng3* mutant also had increased expression levels in the *fng1* mutant (Fig. 3b). These results indicated that subsets of genes were co-regulated by Fng1 and Fng3 in *F. graminearum*.

Deletion of *FNG3* also affects H4 acetylation

Fng3 appears to co-regulate subsets of genes with Fng1, a NuA4 component, we then assayed H4 acetylation in the *fng3* mutant. Proteins were extracted from vegetative hyphae and assayed for

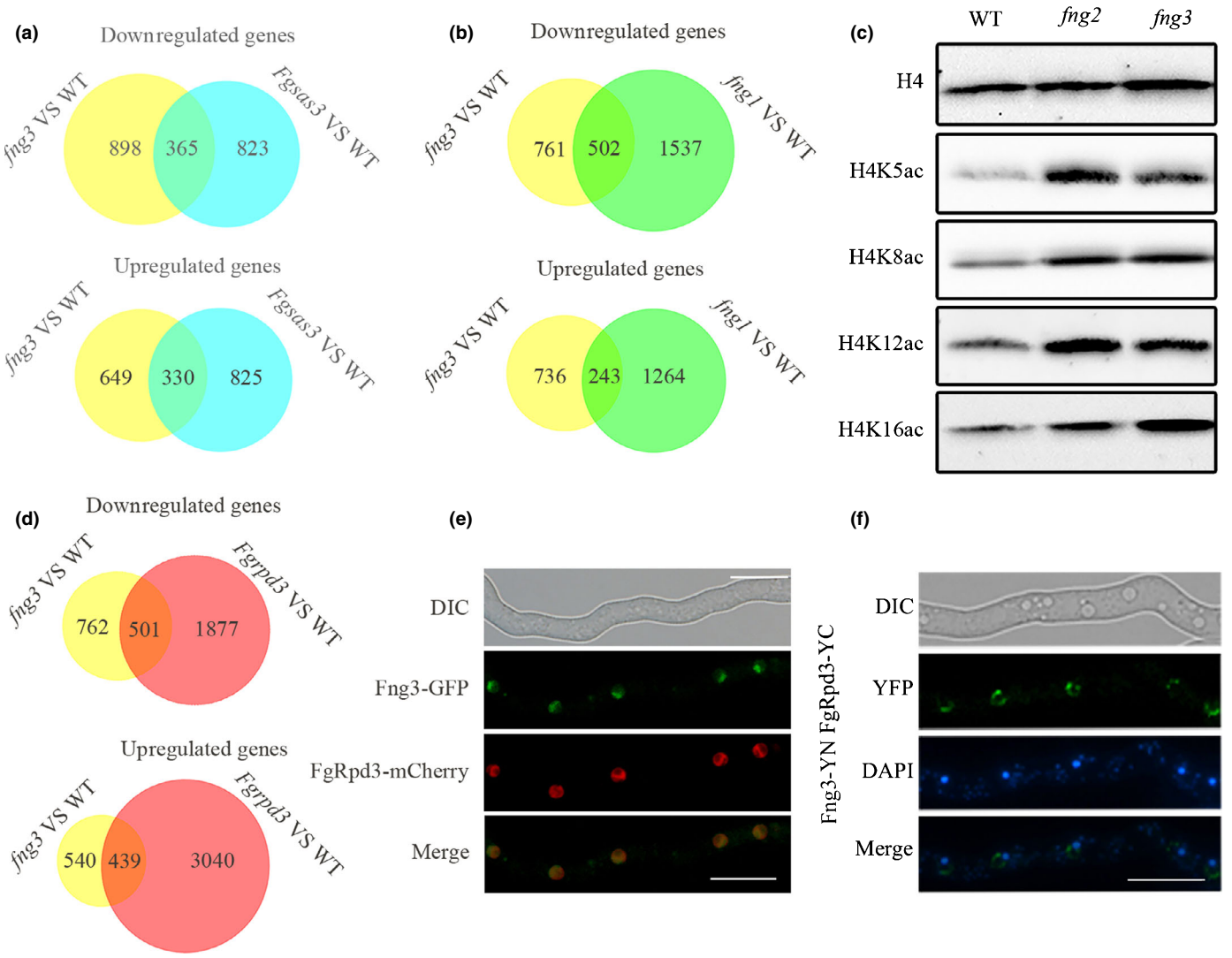

Fig. 3 Association of Fng3 with the FgRpd3 histone deacetylase (HDAC) complex for the regulation of H4 deacetylation and gene expression. (a) Venn diagram showing the numbers of differentially expressed genes (DEGs) downregulated (upper panel) and upregulated (lower panel) in the *fng3* and *Fgsas3* mutants. Upper panel ($P < 3.195e{-}114$), Lower panel ($P < 1.858e{-}127$). The *P*-value for hypergeometric test indicated the overlap of DEGs between different RNA-seq data is significant. (b) Venn diagram showing the numbers of DEGs downregulated (upper panel) and upregulated (lower panel) in the *fng3* and *fng1* mutants. Upper panel ($P < 8.043e{-}121$), lower panel ($P < 3.544e{-}39$). (c) Western blots of total proteins isolated from the wild-type (WT) and the *fng2* and *fng3* mutants were detected with the antibodies specific for H4K5ac, H4K8ac, H4K12ac and H4K16ac. (d) Venn diagram showing the number of DEGs downregulated (upper panel) and upregulated (lower panel) in the *fng3* and *FgRpd3* mutants. Upper panel ($P < 5.630e{-}92$), lower panel ($P < 4.352e{-}46$). (e) Germlings of the FNG3-GFP FgRPD3-mCherry transformant were examined by DIC and epifluorescence microscopy. Bar, 10 μm. (f) Bimolecular fluorescence complementation (BiFC) assays for the interaction of Fng3 with FgRpd3. Germlings of the *FNG3*-nYFP *FgRPD3*-cYFP transformant were stained with DAPI and examined by epifluorescence microscopy. YFP, yellow fluorescent protein. Bar, 10 μm.

H4 acetylation with the antibodies specific for H4K5ac, H4K8ac, H4K12ac and H4K16ac. The *fng3* deletion mutant was increased in the acetylation level at all of these four lysine residues of H4, with the highest level at H4K16 (Fig. 3c). These results indicate that deletion of *FNG3*, a component of the NuA3 HAT complex, results in an elevated H4 acetylation. Therefore, Fng3 is not only important for H3 acetylation, but also plays a role in the regulation of H4 deacetylation. As a control, elevated acetylation levels of H4K5ac, H4K8ac, H4K12ac and H4K16ac also were detected in the *fng2* mutant (Fig. 3c). Therefore, both Fng3 and Fng2 are involved in H4 acetylation although only Fng3 is important for H3 acetylation as a NuA3 complex component.

Fng3 also is associated with the Rpd3 HDAC complex

Unlike the *fng1* mutant that has severe growth defects and produces spontaneous suppressors with faster growth rate as a result of mutations in the FgRpd3 complex, the *fng3* mutant has only a minor reduction in growth rate and it was stable. Because suppressor mutations in *FgRPD3* increased H4 acetylation in the *fng1* mutant, it is possible that the effects of *FNG3* deletion on H4 acetylation also are mediated by the FgRpd3 complex. To test this hypothesis, we first examined the expression levels of the genes affected by *FNG3* deletion in RNA-seq data of the *Fgrpd3* mutant (H. Jiang *et al.*, 2020). Among the 1263 and 979 DEGs

that were down- or upregulated in the *fng3* mutant, 501 and 439 of them also were down- or upregulated, respectively, in the *Fgrpd3* mutant (Fig. 3d), suggesting that > 40% of the genes with altered expression levels in the *fng3* mutant may be co-regulated with *FgRPD3*. The 439 DEGs upregulated in both *Fgrpd3* and *fng3* mutants had relatively lower H4ac enrichment than random-selected genes (Fig. S6a). The low level of H4ac enrichment in those genes may be maintained by Fng3 and its related Rpd3 HDAC complex. GO analysis revealed that they were enriched for genes involved in flavin mononucleotide (FMN) binding and metabolic process (Fig. S6b).

We then generated the *FNG3*-GFP and *FgRPD3*-mCherry fusion constructs and transformed them into the WT strain PH-1. In 12-h germ tubes of the resulting transformants, colocalization of GFP and mCherry signals were observed in most nuclei examined (Fig. 3e), suggesting that Fng3-GFP and FgRpd3-mCherry proteins may be associated with each other in the nucleus. To test this hypothesis, the *FNG3*-nYFP and *FgRPD3*-cYFP fusion constructs were generated and transformed into PH-1 for BiFC assays. YFP signals were observed in the resulting transformants expressing both *FNG3*-nYFP and *FgRPD3*-cYFP fusion proteins (Fig. 3f). Although the interaction between Fng3 and FgSas3 was mediated by FgNto1, FgRpd3 failed to interact with FgNto1 in yeast two hybrid assays (Fig. S7a). Furthermore, YFP signals still were observed in the nucleus of *FNG3*-nYFP *FgRPD3*-cYFP transformant when *FgNTO1* was deleted (Fig. S7b). These results indicate that Fng3 may interact with FgRpd3 independent of FgNto1, and is functionally related to the FgRpd3 HDAC complex for H4 acetylation in *F. graminearum*.

The ING domain is responsible for functional specificity of Fng2 and Fng3

In yeast, Pho23 is an ING protein that directly interacts with Rxt2, a component of the Rpd3 HDAC complex (Sardiu *et al.*, 2009). The *F. graminearum* genome has one distinct ortholog of yeast Rxt2 (FGRAMPH1_01T10383). To test whether Fng3 is associated with the FgRpd3 complex by interacting with FgRxt2, we generated the Fng3 bait construct and transformed it together with the FgRxt2 prey construct into yeast strain AH109 (Wagemans & Lavigne, 2015). Yeast transformants expressing the Fng3 bait and FgRxt2 prey constructs failed to grow on SD-His plates (Fig. 4a), indicating that there is no direction interaction between Fng3 and FgRxt2. Because yeast Pho23 is more closely related to Fng2 in *F. graminearum*, we also generated the Fng2 bait construct. Yeast cells expressing the Fng2 bait and FgRxt2 prey constructs could grow on SD-His plates (Fig. 4a). Therefore, Fng2 interacts with FgRxt2, which may affect the FgRpd3 complex and H4 acetylation in *F. graminearum*. Fng3 must interact with other components of the FgRpd3 HDAC complex.

For fungal ING proteins, the C-terminal PHD finger domain is known to bind with trimethylated lysines on histone tails (Shi *et al.*, 2006) but the role of N-terminal ING domain is not clear. To determine its role in protein–protein interactions, we generated chimeric bait constructs in which the N-terminal region with the ING domain were swapped between Fng2 and Fng3 (Fig. 4b). Interestingly, yeast transformants expressing the FgRxt2 prey and Fng3^{NT2} bait constructs grew on SD-His plates. By contrast, the FgRxt2 Fng2^{NT3} transformants failed to grow on SD-His plates (Fig. 4b). These results indicate that the N-terminal region determines the specificity of Fng2 and Fng3 proteins for interacting with FgRxt2.

In order to further characterize the function of ING domains in Fng2 and Fng3, we generated the *FNG2*^{ING3} allele in which the ING domain of Fng2 was replaced with that of Fng3 and transformed it into the *fng2* mutant. The resulting transformant had similar growth defects with the *fng2* mutant (Fig. 4c). We also generated the *FNG2*^{PHD3} allele in which the PHD region of Fng2 was replaced with that of *FNG3* and transformed it into the *fng2* mutant. The resulting transformant was normal in vegetative growth (Fig. 4c). Likewise, the *FNG3*^{PHD2} but not *FNG3*^{ING2} allele complemented the defect of the *fng3* mutant in vegetative growth (Fig. 4c). Therefore, the PHD domain must be responsible for the reader function in both Fng2 and Fng3 proteins. However, the ING domain determines which proteins they interact with, and with which protein complex they are associated.

The C-terminal region of FgRpd3 mediates its interaction with Fng3

Three yeast ING proteins are associated with three different histone-modifying complexes, yet Fng3 is associated with both FgSas3 NuA3 HAT and FgRpd3 HDAC complexes in *F. graminearum*. Unlike Fng3 orthologs with relatively conserved sequences, we noticed that FgRpd3 has a C-terminal tail region (FgRpd3^{CT}, 440–649 aa) that is not present in yeast Rpd3 although they have similar N-terminal regions (NT) with the HDAC domain (Fig. 5a). FgRpd3 orthologs from other filamentous ascomycetes, such as *Neurospora crassa* and *Magnaporthe oryzae*, also have this extra C-terminal tail region (Fig. 5a). To characterize its role in the interaction of FgRpd3 with Fng3, the *FgRPD3*^{CT}-nYFP and *FNG3*-cYFP fusion constructs were generated and transformed into PH-1. In the resulting transformants, YFP signals were observed in the nucleus (Fig. 5b). For comparison, we also generated the *FgRPD3*^{NT}-nYFP and yeast RPD3-nYFP fusion constructs and co-transformed them with *FNG3*-cYFP into PH-1. YFP signals were not detected in the resulting *FgRPD3*^{NT}-nYFP *FNG3*-cYFP (Fig. 5b) and yeast *RPD3* nYFP *FNG3*-cYFP transformants (Fig. 5c). These results indicate that Fng3 interacts with FgRpd3 via its C-terminal tail region.

In order to test whether this C-terminal tail region of FgRpd3 has as a conserved role in its interaction with Fng3, we also generated the *MoRPD3*^{CT}-nYFP and *NcRPD3*^{CT}-nYFP fusion constructs (Fig. 5a) and co-transformed them with *FNG3*-cYFP into PH-1, respectively. YFP signals were observed in the nucleus in transformants of PH-1 expressing the *FNG3*-cYFP and *MoRPD3*^{CT}-nYFP or *NcRPD3*^{CT}-nYFP fusion constructs (Fig. 5d). Therefore, although they only share < 30% identity in amino acid sequences (Fig. S8), the C-terminal tail regions of FgRpd3 and its orthologs from *M. oryzae* and *N. crassa* have a

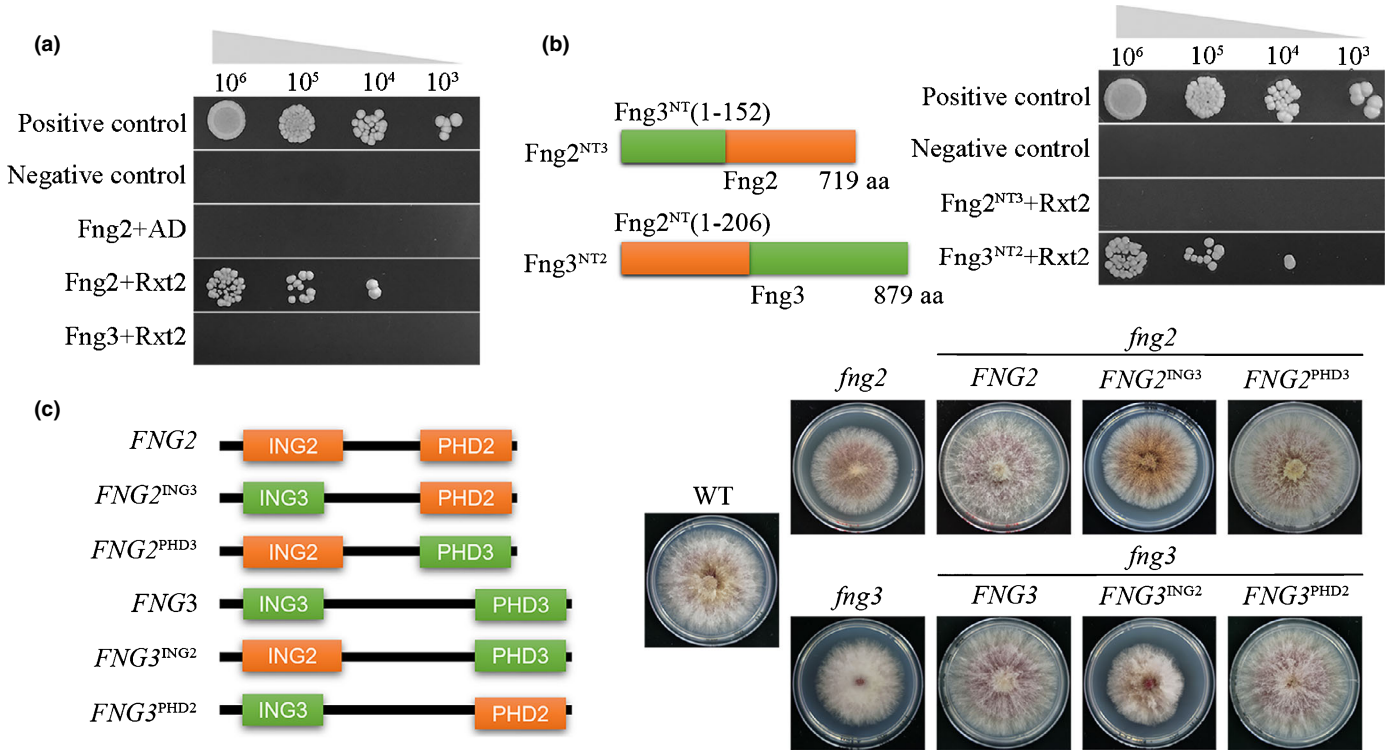

Fig. 4 Functional characterization of the INhibitor of Growth (ING) domains of Fng3 and Fng2. (a) Different concentrations (cells ml^{-1}) of yeast transformants expressing the indicated bait and prey constructs were assayed for growth on SD-His plates. (b) Yeast cells expressing the FgRxt2 prey and $Fng2^{NT3}$ or $Fng3^{NT2}$ bait constructs with their ING domain region swapped as depicted on the left were assayed for growth on SD-His plates. (c) Three-day-old potato dextrose agar (PDA) cultures of the wild-type (WT) and transformants of the *fng2* (upper right) and *fng3* (lower right) mutants expressing different chimeric alleles of *FNG2* and *FNG3* with their ING and PHD domains swapped as depicted on the left.

conserved role in interacting with Fng3 ING proteins, probably for H4 modifications.

Phase separation of the intrinsically disordered regions of $FgRpd3^{CT}$ may assist its binding with Fng3

Interestingly, the C-terminal tail of FgRpd3 ($FgRpd3^{CT}$) is interspersed with intrinsically disordered regions (IDRs) (Fig. 6a), probably exhibiting characteristics of liquid-like condensates. To examine the dynamics of $FgRpd3^{CT}$, we performed FRAP assays with hyphae of the *FgRPD3*^{CT}-GFP transformant. After photobleaching, $FgRpd3^{CT}$-GFP puncta recovered fluorescence on a time scale of seconds (Fig. 6b), indicating that $FgRpd3^{CT}$ can undergo phase separation.

In order to determine whether $FgRpd3^{CT}$ exhibits liquid-like properties *in vitro*, we purified the $FgRpd3^{CT}$-GFP fusion proteins expressed in *Escherichia coli*. Recombinant $FgRpd3^{CT}$-GFP proteins were soluble and did not form droplets in the absence of the crowding agent PEG8000 (Fig. 6c). However, addition of 10% PEG8000 to mimic the molecular crowding that occurs in cells resulted in droplet formation in a $FgRpd3^{CT}$-GFP protein concentration-dependent manner (Fig. 6c). In addition, we observed that two droplets readily fused into a larger droplet once they came in close proximity (Fig. 6d). FRAP of a small area within the droplet was followed by rapid recovery, reflecting local rearrangement of $FgRpd3^{CT}$ molecules within the condensate (Fig. 6e). These dynamic and reversible events suggest that $FgRpd3^{CT}$ undergoes phase separation to form liquid condensates *in vitro*.

The aliphatic alcohol 1,6-hexanediol (1,6-Hex) is known to inhibit weak hydrophobic interactions that are favorable for phase separation (Long *et al.*, 2021). To test its effects on FgRpd3 and its interaction with Fng3 *in vivo*, we treated germlings of the $FgRpd3^{CT}$-nYFP FNG3-cYFP transformant with 5% 1,6-hexanediol. After 2 h treatment, YFP signals were no longer visible (Fig. S9a). As a control, 1,6-Hex treatment did not abolish the interaction between Fng2 and FgRpd3 based on BiFC assays (Fig. S9b). These results indicate that the interaction of $FgRpd3^{CT}$ with Fng3 was disrupted by 1,6-hexanediol (Fig. S9), probably due to its inhibition of phase separation in the IDRs of $FgRpd3^{CT}$ and weak hydrophobic interactions with Fng3.

A short segment in the middle region of Fng3 mediates the interaction of Fng3 with FgRpd3 but not FgSas3

In comparison with its yeast ortholog, Fng3 has an extra 268-aa region in its middle region. Sequence alignment showed that two short segments (601–613 and 728–746 aa) in this middle region are conserved in Fng3 and its orthologs from *M. oryzae* and *N. crassa* (Fig. S10a). In BiFC assays, deletion of the 601–613 aa region resulted in a loss of Fng3–FgRpd3 interaction but had no

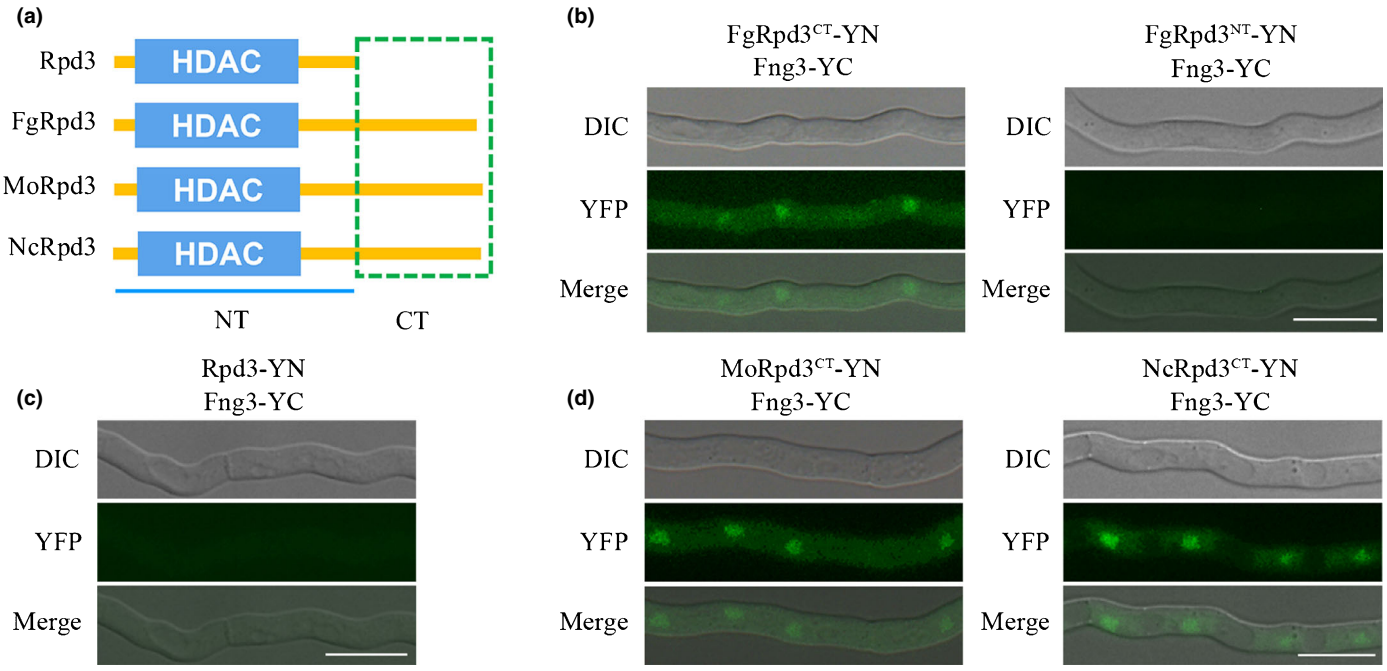

Fig. 5 Roles of the C-terminal extension of FgRpd3 in its interaction with Fng3. (a) Schematic drawing of yeast Rpd3 and its orthologs from *Fusarium graminearum*, *Magnaporthe oryzae* and *Neurospora crassa*. NT, N-terminal region with the HDAC domain; CT, divergent C-terminal tail region. (b) Bimolecular fluorescence complementation (BiFC) assays for the interaction of Fng3 with the CT and NT regions of FgRpd3. Germlings of transformants expressing the *FNG3*-cYFP and *FgRPD3*^{CT} nYFP or *FgRPD3*^{NT}-nYFP constructs were examined for YFP signals by epifluorescence microscopy. YFP, yellow fluorescent protein. Bar, 10 μm. (c) BiFC assays for the interaction of Fng3 with yeast Rpd3. Germlings of transformants expressing yeast *RPD3*^{CT}-nYFP and *FNG3*-cYFP constructs were examined for YFP signals by epifluorescence microscopy. Bar, 10 μm. (d) BiFC assays for the interaction of Fng3 with the C-terminal tail of MoRpd3 (*M. oryzae*) and NcRpd3 (*N. crassa*). Germlings of transformants expressing the *FNG3*-cYFP and *MoRPD3*^{CT}-nYFP or *NcRPD3*^{CT}-nYFP constructs were examined for YFP signals by epifluorescence microscopy. Bar, 10 μm.

effect on the Fng3–FgSas3 interaction. By contrast, the 728–746 aa region of Fng3 was dispensable for its interaction with both FgRpd3 or FgSas3 (Fig. S10b).

In order to verify its importance in the Fng3–FgRpd3 interaction *in vivo*, we then generated the *FNG3*$^{\Delta 601–613aa}$ construct and transformed it into the *fng3* mutant. The resulting *fng3*/*FNG3*$^{\Delta 601–613aa}$ transformant had a higher H4 acetylation level than the WT, indicating that disruption of the interaction between Fng3 and FgRpd3 might reduce the deacetylase activity of FgRpd3 (Fig. S10c). However, although the *fng3* deletion mutant was defective in H3K14 acetylation, the *fng3*/*FNG3*$^{\Delta 601–613aa}$ transformant had a slightly increased H3K14ac level in comparison with the WT (Fig. S10c). These results suggested an equilibrium between NuA3 HAT and Rpd3 HDAC activities. When the Fng3–FgRpd3 interaction is disrupted, FgSas3 might recruit more Fng3 to enhance its HAT activity. When cultured on PDA medium, no obvious defects were observed in the resulting *fng3*/*FNG3*$^{\Delta 601–613aa}$ transformant in comparison with the WT (Fig. S10d). Therefore, it is likely that the growth defect of the *fng3* mutant probably was related to reduced NuA3 HAT activities.

Discussion

Histone acetyltransferases and HDACs generally reside in multiprotein complexes that are composed of various subunits with different functions, including the regulation of HAT/HDAC activities, histone substrate selection and recruitment of HAT/HDAC complexes to specific genomic regions (Lee & Workman, 2007). ING proteins often act as epigenome readers in the HAT or HDAC complexes (Shi *et al.*, 2006; Taverna *et al.*, 2006). In this study, we showed that Fng3, not Fng2, is associated with the NuA3 complex (Fig. 7a). Therefore, like its yeast ortholog Yng1, Fng3 is the ING protein of the NuA3 complex in *F. graminearum*. Although the yeast *yng1* mutant had no obvious defects (Loewith *et al.*, 2000), the *fng3* deletion mutant is defective in vegetative growth, conidiation, asexual development, pathogenesis and DON production. *FNG3* orthologs are unique to ascomycetes but have not been functionally characterized in any other fungi. In *F. graminearum*, deletion of *FNG3* affected H3 acetylation, particularly the acetylation of H3K4, H3K14 and H3K36, which is consistent with an earlier report on the role of *FgSAS3* that encodes the HAT of the NuA3 complex (Kong *et al.*, 2018). Although direct interaction between Fng3 and FgSas3 was not detected, both interacted with FgNto1, a subunit of NuA3 HAT complex (Fig. 7b). Deletion of *FgNTO1* in *F. graminearum* disrupted the association of Fng3 with FgSas3, suggesting a scaffolding role of FgNto1. In yeast, Nto1 affects the stability of Sas3 proteins (Lenstra *et al.*, 2011) and has a weak affinity for H3K36me3 (Shi *et al.*, 2007), but its role as a scaffold protein to mediate the integrity of NuA3 HAT complex has not been reported.

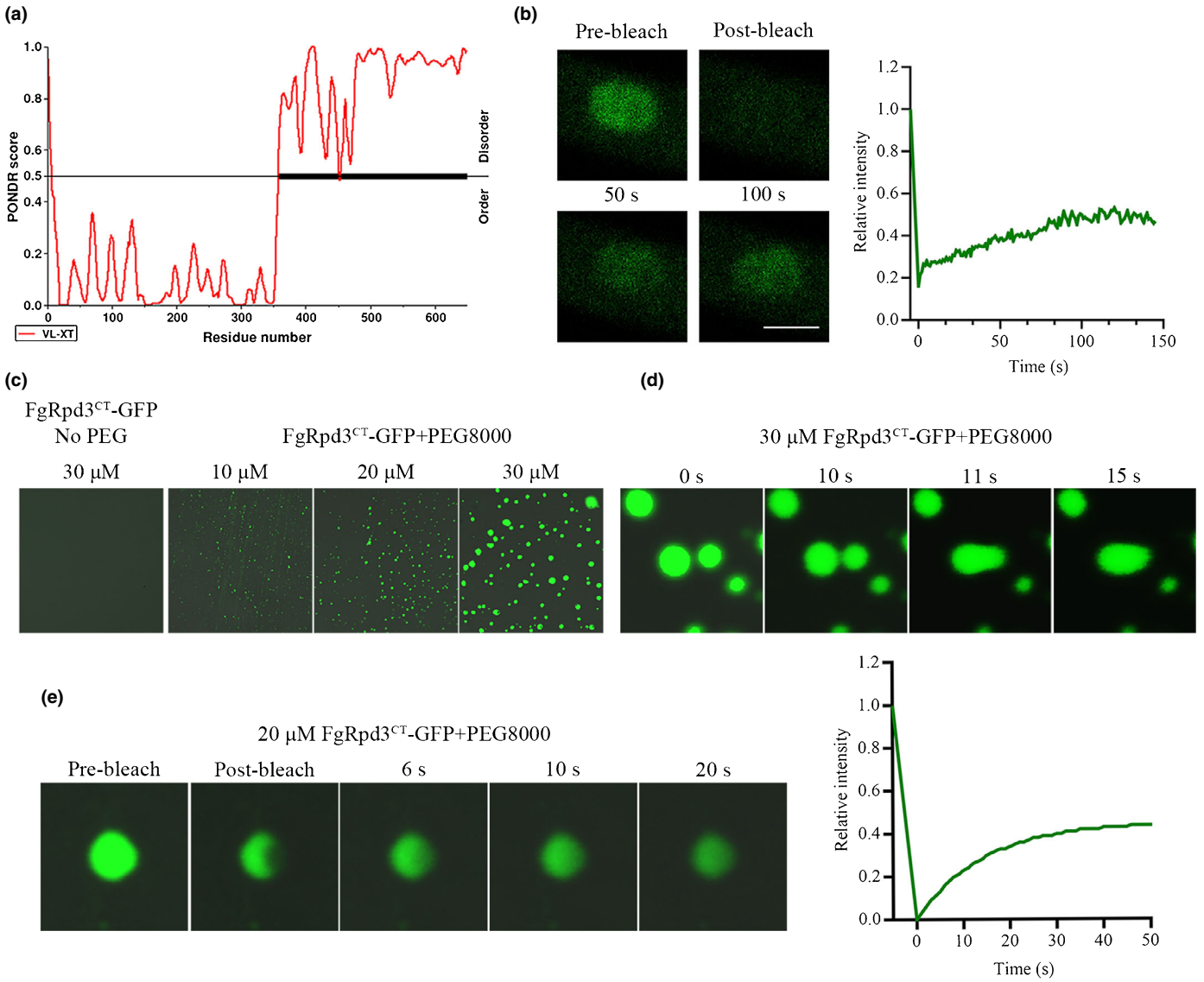

Fig. 6 Phase separation of the C-terminal extension of FgRpd3. (a) Intrinsically disordered regions (IDRs) in the C-terminal extension (440–649 aa) of FgRpd3 identified by PONDR (Predictor of Natural Disordered Regions) program with the PONDR score > 0.5. (b) Representative Fluorescence recovery after photobleaching (FRAP) images (left panels) and quantitative measures (right panels) of green fluorescent protein (GFP) signals in the nucleus inside hyphae of the *FgRPD3*^{CT}-GFP transformant. Bar, 2 μm. The pre-bleaching image was taken 3 s before bleaching. Other images were taken immediately (0) and 50 or 100 s after bleaching. Relative intensity of GFP signals at different post-bleaching time points was estimated with the pre-bleach point as 1. (c) Representative images of recombinant *FgRPD3*^{CT}-GFP proteins purified from *Escherichia coli* at the marked concentrations with or without (CK) 10% PEG8000. Bar, 10 μm. (d) Representative images at different time points showing the dynamic fusion of liquid droplets containing FgRpd3^{CT}-GFP *in vitro*. Bar, 2 μm. (e) Representative FRAP images (left panels) and quantitative measures (right panels) of the recovered fluorescence intensity in the bleached region to show the fluidity of *FgRPD3*^{CT}-droplets. Bar, 2 μm.

Interestingly, we found that Fng3 also interacted with the FgRpd3 HDAC to mediate H4 deacetylation in *F. graminearum* (Fig. 7a). In yeast, Yng1 and Pho23 are functionally associated with the NuA3 HAT and Rpd3 HDAC complexes, respectively. We found that, Fng2, like its yeast ortholog Pho23, also interacted with the FgRpd3 HDAC complex. However, Fng2 and Fng3 differed in their associations with the FgRpd3 complexes. Whereas Fng2 interacted with FgRxt2, which is similar to the interaction of Pho23 with Rxt2 in the yeast Rpd3 complex (Sardiu *et al.*, 2009), direct interaction between Fng3 and FgRxt2 was not observed (Fig. 7b). Instead, we found that Fng3 interacted with FgRpd3. Therefore, Fng3 appears to be associated with both the NuA3 HAT and FgRpd3 HDAC complexes in *F. graminearum* (Fig. 7a). To the best of our knowledge, no ING protein has been reported to interact with two distinct histone modification complexes in fungi. In *F. graminearum*, the FgRpd3 HDAC is involved in regulating H4 acetylation (H. Jiang *et al.*, 2020). The direct interaction of Fng3 with FgRpd3 may explain why deletion of *FNG3*, a component of NuA3 complex, resulted in defects in H4 acetylation. A short segment in the middle region of Fng3 was specifically required for the interaction between Fng3 and FgRpd3. The NuA3 complex may recruit

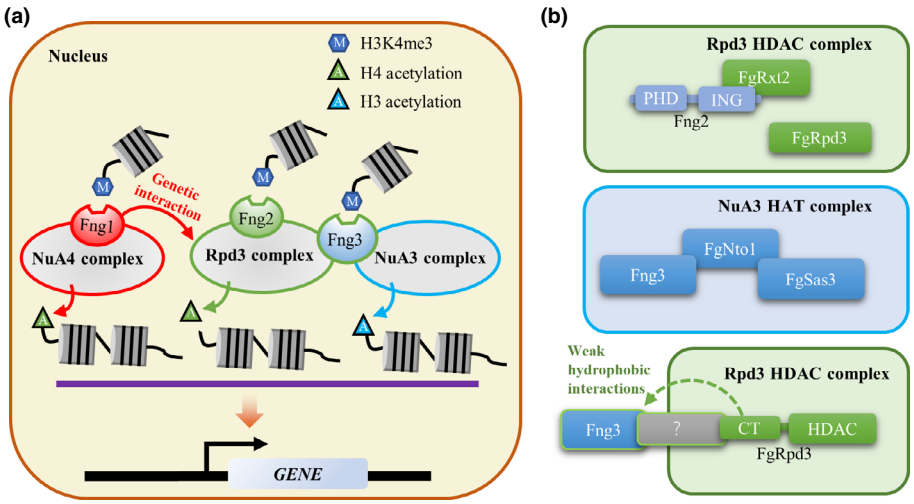

Fig. 7 A schematic model for regulation of histone acetylation by INhibitor of Growth (ING) proteins in *Fusarium graminearum*. (a) Roles of ING proteins in histone acetylation and deacetylation. Fng1 physically interacts with NuA4 histone acetyltransferase (HAT) complex to regulate H4 acetylation and also genetically interacts with the Rpd3 histone deacetylase (HDAC) complex. Fng2 tends to be a subunit of Rpd3 HDAC complex for the regulation of H4 deacetylation. Fng3 interacts with both the NuA3 HAT complex and Rpd3 HDAC complex, and probably plays an important role in balance of H3 acetylation and H4 deacetylation. (b) ING proteins interact with histone-modifying complexes through different way. Fng2 binds with FgRxt2, a component of Rpd3 HDAC complex. The N-terminal ING domain is required for the interaction. Fng3 interacts with FgSas3 in the presence of FgNto1, and also established an association with the C-terminus of FgRpd3, probably though weak hydrophobic interactions.

more Fng3 to enhance the FgSas3 HAT activity when the interaction between Fng3 and FgRpd3 was disrupted, suggests an equilibrium between NuA3 HAT and Rpd3 HDAC activities. In comparison with yeast Rpd3, FgRpd3 and its orthologs from *N. crassa* (Smith *et al.*, 2010) and *M. oryzae* (Lee *et al.*, 2021) have an extra C-terminal tail region that is unique to filamentous ascomycetes. Further characterization showed that the C-terminal region of FgRpd3 was responsible for its interaction with Fng3 (Fig. 7b). Unlike the N-terminal HDAC domain, the amino acid sequences of the C-terminal tail of FgRpd3 orthologs are not well-conserved in filamentous fungi. However, the C-terminal tail of FgRpd3 orthologs from *M. oryzae* and *N. crassa* also interacted with Fng3, indicating that it has a conserved role in the interaction of Rpd3 with Fng3. One possible explanation is that differences in aa sequences may not affect the folding or function of the C-terminal tail of FgRpd3 orthologs and interactions with Fng3 ING proteins. MoRpd3 was able to complement yeast deletion mutant of Rpd3. Whereas MoRpd3 without C-terminal tail could only partially do (Lee *et al.*, 2021), suggests the C-terminal tail of MoRpd3 is not limited to provide platform for interaction with other proteins such as Fng3. Indeed, multiple frame-shift mutation in the C-terminal region of FgRpd3 was suppressive to the *fng1* mutant in *F. graminearum*, indicated that the C-terminal region of FgRpd3 also was functionally related to Fng1 (H. Jiang *et al.*, 2020). In *C. albicans*, Rpd3 and Rpd31 are two paralogous histone deacetylases that play opposite roles in regulating the white-opaque switching (Xie *et al.*, 2016). However, only Rpd31, similar to FgRpd3, has a longer C-terminal tail region than yeast Rpd3. It is possible that the functional difference between Rpd3 and Rpd31 is related to their interactions with different ING proteins in *C. albicans*.

The ING domain is the hallmark of ING proteins (Loewith *et al.*, 2000; Gordon *et al.*, 2008) but its exact function is not well-characterized. In this study, we showed that the ING domain of Fng2 is responsible for its interaction with FgRxt2 and functional specificity. Replacing the ING domain of Fng3 with that of Fng2 led to its interaction with FgRxt2. Furthermore, swapping the ING domain between *FNG2* and *FNG3* enabled the chimeric $FNG2^{ING3}$ and $FNG3^{ING2}$ alleles of to cross-complement the *fng3* and *fng2* deletion mutants. Sequence alignment analysis showed that the ING domain of Fng2 and its closely related orthologs has a 47-aa region that is absent in Fng3 orthologs. This extra region in the Fng2 may play an important role in the functional differences between Fng2 and Fng3, probably in determining the proteins or protein complexes they interact with.

Overall, Fng3 appears to be associated with both the NuA3 HAT and FgRpd3 HDAC complexes in *F. graminearum* (Fig. 7a). Fng3 has a conserved PHD finger domain in its C-terminal region, which probably functions as a histone H3K4me3-binding module (Sanchez & Zhou, 2011). With this chromatin binding module, Fng3 may recruit and mediate the spatiotemporal assembly of the Nua3 HAT and Rpd3 HDAC complexes to the H3K4-methylated chromatins for dynamic regulation of histone acetylation and deacetylation and gene expression in *F. graminearum*. In yeast, Yng1 is a component of NuA3 complex but it is not known to interact with Rpd3. Nevertheless, the NuA3 HAT complex antagonizes the Rpd3 HDAC to optimize mRNA and lncRNA expression dynamics with its distinct chromatin readers, such as Yng1, Nto1 and Pdp3 (Kim *et al.*, 2020). The association of Fng3 with two distinct histone modifying complexes represent a novel chromatin regulation in *F. graminearum* and other fungi. It is possible that difference in the affinities of Fng3 with its interacting proteins (such as FgNto1 and FgRpd3) is important to determine their interactions and spatiotemporal regulation of the NuA3 HAT and FgRpd3

HDAC activities. Similar to Fng3, yeast Taf14, a chromatin reader identified in multiple protein complexes, binds to the acetylated lysine markers on the chromatins with its YEATS domain and serves as an organization hub to orchestrate transcription machinery recruitment (Andrews *et al.*, 2016; Peil *et al.*, 2020). The scaffolding role of Taf14 is required for phase separation of transcription machineries, thereby ensuring efficient spatiotemporal control of transcription (Chen *et al.*, 2020). In *F. graminearum*, Fng3 may play a similar role to promote the phase separation of the NuA3 and RPD3 complexes.

Acknowledgements

We thank Hua Zhao, Fengping Yuan, Guoyun Zhang, Ping Xiang and Jie Liang for assistance with microscopic examinations and DON measurement, and Xue Zhang, Guanghui Wang, Chenfang Wang, Ming Xu and Zhe Tang for fruitful discussions. This work was supported by grants from National Natural Science Foundation of China (nos. 32172378, 32102181, 31801688), Shaanxi Science Fund for Distinguished Young Scholars (2022JC-14) and the National Youth Talent Support Program to CJ as well as a grant to JRX from the USWBSI.

Competing interests

None declared.

Author contributions

CJ planned and designed the research; HX, MY, AX, HJ and PH performed experiments; HL, RH, DAL and QW analyzed data; and CJ and J-RX wrote the manuscript. HX, MY and AX contributed equally to this work.

ORCID

Rui Hou https://orcid.org/0000-0003-4056-6140
Panpan Huang https://orcid.org/0000-0001-9052-004X
Cong Jiang https://orcid.org/0000-0002-5634-3200
Hang Jiang https://orcid.org/0000-0002-8361-8206
Dongao Li https://orcid.org/0000-0002-9367-122X
Huiquan Liu https://orcid.org/0000-0002-4723-845X
Qinhu Wang https://orcid.org/0000-0003-1251-073X
Aliang Xia https://orcid.org/0000-0002-5045-7389
Huaijian Xu https://orcid.org/0000-0003-1292-1678
Jin-Rong Xu https://orcid.org/0000-0001-5999-5004
Meng Ye https://orcid.org/0000-0002-5520-7434

Data availability

All relevant data are within the paper and its Supporting Information files. RNA-seq data generated in this study were deposited at the NCBI SRA database under accession nos. SRR17659995–SRR17660003, SRR19214415–SRR19214418 and SRR19414282–SRR19414283.

References

Andrews FH, Shinsky SA, Shanle EK, Bridgers JB, Gest A, Tsun IK, Krajewski K, Shi XB, Strahl BD, Kutateladze TG. 2016. The Taf14 YEATS domain is a reader of histone crotonylation. *Nature Chemical Biology* **12**: 396–398.

Audenaert K, Vanheule A, Hofte M, Haesaert G. 2013. Deoxynivalenol: a major player in the multifaceted response of Fusarium to its environment. *Toxins* **6**: 1–19.

Boenisch MJ, Schafer W. 2011. *Fusarium graminearum* forms mycotoxin producing infection structures on wheat. *BMC Plant Biology* **11**: 110.

Bruno KS, Tenjo F, Li L, Hamer JE, Xu JR. 2004. Cellular localization and role of kinase activity of PMK1 in *Magnaporthe grisea*. *Eukaryotic Cell* **3**: 1525–1532.

Chen GC, Wang D, Wu B, Yan FX, Xue HJ, Wang QM, Quan S, Chen Y. 2020. Taf14 recognizes a common motif in transcriptional machineries and facilitates their clustering by phase separation. *Nature Communications* **11**: 4206.

Chen JQ, Li Y, Pan X, Lei BK, Chang C, Liu ZX, Lu H. 2010. The fission yeast inhibitor of growth (ING) protein Png1p functions in response to DNA damage. *Journal of Biological Chemistry* **285**: 15786–15793.

Chen Y, Kistler HC, Ma Z. 2019. *Fusarium graminearum* trichothecene mycotoxins: biosynthesis, regulation, and management. *Annual Review of Phytopathology* **57**: 15–39.

Choy JS, Tobe BTD, Huh JH, Kron SJ. 2001. Yng2p-dependent NuA4 histone H4 acetylation activity is required for mitotic and meiotic progression. *Journal of Biological Chemistry* **276**: 43653–43662.

Connolly LR, Smith KM, Freitag M. 2013. The *Fusarium graminearum histone* H3 K27 methyltransferase KMT6 regulates development and expression of secondary metabolite gene clusters. *PLoS Genetics* **9**: e1003916.

Cuomo CA, Gueldener U, Xu JR, Trail F, Turgeon BG, Di Pietro A, Walton JD, Ma LJ, Baker SE, Rep M *et al.* 2007. The *Fusarium graminearum* genome reveals a link between localized polymorphism and pathogen specialization. *Science* **317**: 1400–1402.

Cuzick A, Urban M, Hammond-Kosack K. 2008. *Fusarium graminearum* gene deletion mutants *map1* and *tri5* reveal similarities and differences in the pathogenicity requirements to cause disease on *Arabidopsis* and wheat floral tissue. *New Phytologist* **177**: 990–1000.

Dimont E, Shi J, Kirchner R, Hide W. 2015. EDGERUN: an R package for sensitive, functionally relevant differential expression discovery using an unconditional exact test. *Bioinformatics* **31**: 2589–2590.

Gale LR, Ward TJ, Balmas V, Kistler HC. 2007. Population subdivision of *Fusarium graminearum* sensu stricto in the upper midwestern United States. *Phytopathology* **97**: 1434–1439.

Gong W, Suzuki K, Russell M, Riabowol K. 2005. Function of the ING family of PHD proteins in cancer. *The International Journal of Biochemistry & Cell Biology* **37**: 1054–1065.

Gordon PM, Soliman MA, Bose P, Trinh Q, Sensen CW, Riabowol K. 2008. Interspecies data mining to predict novel ING-protein interactions in human. *BMC Genomics* **9**: 426.

Goswami RS, Kistler HC. 2004. Heading for disaster: *Fusarium graminearum* on cereal crops. *Molecular Plant Pathology* **5**: 515–525.

Greenstein RA, Barrales RR, Sanchez NA, Bisanz JE, Braun S, Al-Sady B. 2020. Set1/COMPASS repels heterochromatin invasion at euchromatic sites by disrupting Suv39/Clr4 activity and nucleosome stability (vol 34, pg 99, 2020). *Genes & Development* **34**: 1106.

He GHY, Helbing CC, Wagner MJ, Sensen CW, Riabowol K. 2005. Phylogenetic analysis of the ING family of PHD finger proteins. *Molecular Biology and Evolution* **22**: 104–116.

Hou Z, Xue C, Peng Y, Katan T, Kistler HC, Xu JR. 2002. A mitogen-activated protein kinase gene (MGV1) in *Fusarium graminearum* is required for female fertility, heterokaryon formation, and plant infection. *Molecular Plant–Microbe Interactions* **15**: 1119–1127.

Howe L, Kusch T, Muster N, Chaterji R, Yates JR, Workman JL. 2002. Yng1p modulates the activity of Sas3p as a component of the yeast

NuA3 histone acetyltransferase complex. *Molecular and Cellular Biology* **22**: 5047–5053.

Imboden L, Afton D, Trail F. 2018. Surface interactions of *Fusarium graminearum* on barley. *Molecular Plant Pathology* **19**: 1332–1342.

Jansen C, von Wettstein D, Schafer W, Kogel KH, Felk A, Maier FJ. 2005. Infection patterns in barley and wheat spikes inoculated with wild-type and trichodiene synthase gene disrupted *Fusarium graminearum*. *Proceedings of the National Academy of Sciences, USA* **102**: 16892–16897.

Jiang C, Cao SL, Wang ZY, Xu HJ, Liang J, Liu HQ, Wang GH, Ding MY, Wang QH, Gong C *et al.* 2019. An expanded subfamily of G-protein-coupled receptor genes in *Fusarium graminearum* required for wheat infection. *Nature Microbiology* **4**: 1582–1591.

Jiang C, Hei RN, Yang Y, Zhang SJ, Wang QH, Wang W, Zhang Q, Yan M, Zhu GR, Huang PP *et al.* 2020. An orphan protein of *Fusarium graminearum* modulates host immunity by mediating proteasomal degradation of TaSnRK1 alpha. *Nature Communications* **11**: 4382.

Jiang C, Zhang C, Wu C, Sun P, Hou R, Liu H, Wang C, Xu JR. 2016. TRI6 and TRI10 play different roles in the regulation of deoxynivalenol (DON) production by cAMP signalling in *Fusarium graminearum*. *Environmental Microbiology* **18**: 3689–3701.

Jiang H, Xia AL, Ye M, Ren JY, Li DG, Liu HQ, Wang QH, Lu P, Wu CL, Xu JR *et al.* 2020. Opposing functions of Fng1 and the Rpd3 HDAC complex in H4 acetylation in *Fusarium graminearum*. *PLoS Genetics* **16**: e1009185.

Kim JH, Yoon CY, Jun Y, Lee BB, Lee JE, Ha SD, Woo H, Choi A, Lee S, Jeong W *et al.* 2020. NuA3 HAT antagonizes the Rpd3S and Rpd3L HDACs to optimize mRNA and lncRNA expression dynamics. *Nucleic Acids Research* **48**: 10753–10767.

Kong XJ, van Diepeningen AD, van der Lee TAJ, Waalwijk C, Xu JS, Xu J, Zhang H, Chen WQ, Feng J. 2018. The *Fusarium graminearum* histone acetyltransferases are important for morphogenesis, DON biosynthesis, and pathogenicity. *Frontiers in Microbiology* **9**: 654.

Koulouras G, Panagopoulos A, Rapsomaniki MA, Giakoumakis NN, Taraviras S, Lygerou Z. 2018. EasyFRAP-web: a web-based tool for the analysis of fluorescence recovery after photobleaching data. *Nucleic Acids Research* **46**(W1): W467–W472.

Lee KK, Workman JL. 2007. Histone acetyltransferase complexes: one size doesn't fit all. *Nature Reviews Molecular Cell Biology* **8**: 284–295.

Lee SH, Farh ME, Lee J, Oh YT, Cho E, Park J, Son H, Jeon J. 2021. A histone deacetylase, *Magnaporthe oryzae* RPD3, regulates reproduction and pathogenic development in the rice blast fungus. *MBio* **12**: e0260021.

Lenstra TL, Benschop JJ, Kim T, Schulze JM, Brabers NA, Margaritis T, van de Pasch LA, van Heesch SA, Brok MO, Groot Koerkamp MJ *et al.* 2011. The specificity and topology of chromatin interaction pathways in yeast. *Molecular Cell* **42**: 536–549.

Liu H, Zhang S, Ma J, Dai Y, Li C, Lyu X, Wang C, Xu JR. 2015. Two Cdc2 kinase genes with distinct functions in vegetative and infectious hyphae in *Fusarium graminearum*. *PLoS Pathogens* **11**: e1004913.

Loewith R, Meijer M, Lees-Miller SP, Riabowol K, Young D. 2000. Three yeast proteins related to the human candidate tumor suppressor p33(ING1) are associated with histone acetyltransferase activities. *Molecular and Cellular Biology* **20**: 3807–3816.

Loewith R, Smith JS, Meijer M, Williams TJ, Bachman N, Boeke JD, Young D. 2001. Pho23 is associated with the Rpd3 histone deacetylase and is required for its normal function in regulation of gene expression and silencing in *Saccharomyces cerevisiae*. *Journal of Biological Chemistry* **276**: 24068–24074.

Long Q, Zhou Y, Wu H, Du S, Hu M, Qi J, Li W, Guo J, Wu Y, Yang L *et al.* 2021. Phase separation drives the self-assembly of mitochondrial nucleoids for transcriptional modulation. *Nature Structural & Molecular Biology* **28**: 900–908.

Lu Y, Su C, Mao XM, PalaRaniga P, Liu HP, Chen JY. 2008. Efg1-mediated recruitment of NuA4 to promoters is required for hypha-specific Swi/Snf binding and activation in *Candida albicans*. *Molecular Biology of the Cell* **19**: 4260–4272.

Nicolas E, Yamada T, Cam HP, Fitzgerald PC, Kobayashi R, Grewal SI. 2007. Distinct roles of HDAC complexes in promoter silencing, antisense suppression and DNA damage protection. *Nature Structural & Molecular Biology* **14**: 372–380.

Nourani A, Howe L, Pray-Grant MG, Workman JL, Grant PA, Cote J. 2003. Opposite role of yeast ING family members in p53-dependent transcriptional activation. *Journal of Biological Chemistry* **278**: 19171–19175.

Peil K, Jurgens H, Luige J, Kristjuhan K, Kristjuhan A. 2020. Taf14 is required for the stabilization of transcription pre-initiation complex in *Saccharomyces cerevisiae*. *Epigenetics & Chromatin* **13**: 24.

Ren J, Zhang Y, Wang Y, Li C, Bian Z, Zhang X, Liu H, Xu J-R, Jiang C. 2022. Deletion of all three MAP kinase genes results in severe defects in stress responses and pathogenesis in *Fusarium graminearum*. *Stress Biology* **2**: 6.

Sanchez R, Zhou MM. 2011. The PHD finger: a versatile epigenome reader. *Trends in Biochemical Sciences* **36**: 364–372.

Sardiu ME, Gilmore JM, Carrozza MJ, Li B, Workman JL, Florens L, Washburn MP. 2009. Determining protein complex connectivity using a probabilistic deletion network derived from quantitative proteomics. *PLoS ONE* **4**: e7310.

Shi XB, Hong T, Walter KL, Ewalt M, Michishita E, Hung T, Carney D, Pena P, Lan F, Kaadige MR *et al.* 2006. ING2 PHD domain links histone H3 lysine 4 methylation to active gene repression. *Nature* **442**: 96–99.

Shi XB, Kachirskaia I, Walter KL, Kuo JHA, Lake A, Davrazou F, Chan SM, Martin DGE, Fingerman IM, Briggs SD *et al.* 2007. Proteome-wide analysis in *Saccharomyces cerevisiae* identifies several PHD fingers as novel direct and selective binding modules of histone H3 methylated at either lysine 4 or lysine 36. *Journal of Biological Chemistry* **282**: 2450–2455.

Smith KM, Dobosy JR, Reifsnyder JE, Rountree MR, Anderson DC, Green GR, Selker EU. 2010. H2B- and H3-specific histone deacetylases are required for DNA methylation in *Neurospora crassa*. *Genetics* **186**: 1207–1216.

Taverna SD, Ilin S, Rogers RS, Tanny JC, Lavender H, Li HT, Baker L, Boyle J, Blair LP, Chait BT *et al.* 2006. Yng1 PHD finger binding to H3 trimethylated at K4 promotes NuA3 HAT activity at K14 of H3 and transcription at a subset of targeted ORFs. *Molecular Cell* **24**: 785–796.

Trail F. 2009. For blighted waves of grain: *Fusarium graminearum* in the postgenomics era. *Plant Physiology* **149**: 103–110.

Wagemans J, Lavigne R. 2015. Identification of protein-protein interactions by standard gal4p-based yeast two-hybrid screening. *Methods in Molecular Biology* **1278**: 409–431.

Wang C, Zhang S, Hou R, Zhao Z, Zheng Q, Xu Q, Zheng D, Wang G, Liu H, Gao X *et al.* 2011. Functional analysis of the kinome of the wheat scab fungus *Fusarium graminearum*. *PLoS Pathogens* **7**: e1002460.

Wang J, Liu C, Chen Y, Zhao Y, Ma Z. 2021. Protein acetylation and deacetylation in plant-pathogen interactions. *Environmental Microbiology* **23**: 4841–4855.

Xie J, Jenull S, Tscherner M, Kuchler K. 2016. The paralogous histone deacetylases Rpd3 and Rpd31 play opposing roles in regulating the white-opaque switch in the fungal pathogen *Candida albicans*. *MBio* **7**: e01807–e01816.

Zhang XW, Jia LJ, Zhang Y, Jiang G, Li X, Zhang D, Tang WH. 2012. In planta stage-specific fungal gene profiling elucidates the molecular strategies of *Fusarium graminearum* growing inside wheat coleoptiles. *Plant Cell* **24**: 5159–5176.

Zhao XH, Xu JR. 2007. A highly conserved MAPK-docking site in Mst7 is essential for Pmk1 activation in *Magnaporthe grisea*. *Molecular Microbiology* **63**: 881–894.

Zhou X, Zhang H, Li G, Shaw B, Xu JR. 2012. The Cyclase-associated protein Cap1 is important for proper regulation of infection-related morphogenesis in *Magnaporthe oryzae*. *PLoS Pathogens* **8**: e1002911.

Zhou XY, Li GT, Xu JR. 2011. Efficient approaches for generating GFP fusion and epitope-tagging constructs in filamentous fungi. *Methods in Molecular Biology* **722**: 199–212.

Supporting Information

Additional Supporting Information may be found online in the Supporting Information section at the end of the article.

Fig. S1 Distribution of INhibitor of Growth proteins across different fungal lineages and maximum-likelihood phylogeny of those proteins.

Fig. S2 Assays for the expression levels of top six differentially expressed genes (three upregulated, three downregulated genes, respectively) in the WT and *fng3* mutant by qRT-PCR.

Fig. S3 GO enrichment analysis of the downregulated differentially expressed genes in the *fng3* mutant.

Fig. S4 GO enrichment analysis of the upregulated differentially expressed genes in the *fng3* mutant.

Fig. S5 H3K14ac enrichment (a) and GO analysis (b) of genes downregulated in both *fng3* and *Fgsas3* mutants.

Fig. S6 The H4ac enrichment (a) and GO analysis (b) of genes upregulated in both *fng3* and *Fgrpd3* mutants.

Fig. S7 Nto1 is not required for the interaction between Fng3 and FgRpd3.

Fig. S8 Multiple sequence alignment of the C-terminal region of yeast Rpd3 and its orthologs in *Fusarium graminearum* (FgRpd3), *Magnaporthe oryzae* (MoRpd3) and *Neurospora crassa* (NcRpd3).

Fig. S9 Treatment of 1,6-hexanediol (1,6-Hex) inhibited Fng3-FgRpd3CT interaction but not Fng2–FgRpd3 interaction.

Fig. S10 Short segment in the middle region of Fng3 mediates the interaction of Fng3 with FgRpd3 but not FgSas3.

Table S1 Wild-type and mutant strains of *Fusarium graminearum* and *Saccharomyces cerevisiae* used in this study.

Table S2 Primers used in this study.

Table S3 Identification of fungal ING genes across different fungal lineages.

Table S4 Identification of DEGs in the *fng3* deletion mutant in comparison with the WT strain PH-1.

Please note: Wiley Blackwell are not responsible for the content or functionality of any Supporting Information supplied by the authors. Any queries (other than missing material) should be directed to the *New Phytologist* Central Office.